MAE 263F HW4

Ursa Z., University of California Los Angeles

***Abstract*— This report presents a numerical study of a helical compression spring modeled as a Discrete Elastic Rod (DER). The goal is to (i) simulate the transient response of a steel helix under a single axial load, (ii) perform a sweep over multiple force levels to extract an effective axial stiffness, and (iii) study how this stiffness scales with coil diameter and compare the results against the textbook formula $k = Gd^4/(8ND^3)$. The rod is discretized into 50 vertices and integrated in time using an implicit Newton iteration with stretching, bending, and twisting energies. For each part, we show the relevant plots: the axial tip displacement versus time, several 3-D snapshots of the deformed helix, the force–displacement curve with a linear fit, and the stiffness–diameter scaling compared with theory. The DER model reproduces the expected linear relation between force and displacement in the small-deflection regime and captures the trend $k \propto D^{-3}$, with moderate quantitative deviations from the textbook prediction at larger diameters.**

I. Introduction

Helical springs are classical structural elements used to store and release elastic energy. Their small-deflection axial stiffness is often estimated using the textbook formula

$$k_{\text{txt}} = \frac{Gd^4}{8ND^3},$$

where G is the shear modulus, d the wire diameter, D the mean coil diameter, and N the number of active turns. While this formula is widely used, it relies on simplifying assumptions such as pure torsion of the wire and small deflections.

In this homework, we use a fully 3-D Discrete Elastic Rod (DER) formulation to simulate the dynamic response of a helical spring under axial loading. The DER model accounts for stretch, bending, and twist of the centerline and uses a dynamic relaxation approach: the spring is given inertia and viscous-like numerical damping, then allowed to evolve until it reaches a steady equilibrium configuration.

II. Methodology

A. Geometry and Material Parameters

The spring consists of a circular wire of radius r0=1mm(d=2r0=2mm) wound into a helix of mean diameter D=0.04m (Part 1 and 2). The helix has N=5 turns and a pitch equal to one wire diameter per turn, so the total axial length is $N \times \text{pitch} = 5 \times 0.002 = 0.01\ \text{m}$. The centerline arc length L is computed from the helix geometry and is approximately 0.628m. The material is taken as nearly incompressible with Young's modulus E=10MPa and Poisson ratio v=0.5, giving shear modulus $G = E/[2(1+\nu)]$. The cross-sectional properties are

$$EA = E\pi r_0^2, EI = \frac{E\pi r_0^4}{4}, GJ = \frac{G\pi r_0^4}{2}.$$

Mass is distributed along the rod assuming density $\rho = 1000\ \text{kg/m}^3$*; a lumped mass vector and diagonal mass matrix are assembled from segment volumes.*

B. Discrete Elastic Rod Formulation

The rod centerline is discretized into $n_v = 50$vertices and $n_e = n_v - 1$edges. The state vector q stores the 3-D position of each vertex and a scalar twist angle θper edge, resulting in $n_{\text{dof}} = 3n_v + n_e$degrees of freedom.
Three elastic energies are considered:

Stretching energy E_s: depends on edge length relative to a reference length, with gradient and Hessian computed by gradEs_hessEs.

Bending energy E_b: depends on curvature $\boldsymbol{\kappa} = (\kappa_1, \kappa_2)$computed from neighboring edges and material directors m_1, m_2. The routine gradEb_hessEb returns its contribution to forces and stiffness.

Twisting energy E_t: depends on integrated twist relative to a reference twist, handled by gradEt_hessEt.
Material frames are transported along the rod using space and time parallel transport to avoid artificial twisting. Curvature and reference twist are updated at each Newton iteration using helper functions such as computeTangent, computeSpaceParallel, computeTimeParallel, getKappa, and getRefTwist.

C. Time Integration and Newton Solver

The equations of motion are advanced with an implicit first-order (backward Euler) scheme. At each time step, the unknown configuration $\mathbf{q}^{n+1}$ is obtained by solving the nonlinear system

$$\mathbf{M}\frac{\mathbf{q}^{n+1}-\mathbf{q}^{n}}{\Delta t^{2}}-\mathbf{M}\frac{\mathbf{u}^{n}}{\Delta t}-\mathbf{F}_{\text{int}}(\mathbf{q}^{n+1})-\mathbf{F}_{\text{ext}}=0,$$

where $\mathbf{F}_{\text{int}}=\mathbf{F}_{s}+\mathbf{F}_{b}+\mathbf{F}_{t}$ and $\mathbf{F}_{\text{ext}}$ is the applied tip load. The function objfun assembles internal forces and Jacobians, then performs Newton iterations on the free degrees of freedom until the maximum update $|\Delta\mathbf{q}|$ falls below a tolerance proportional to the segment length.

II. Results and Discussion

A. Part 1 – Single Load Level $F=F_{\text{char}}$

The characteristic force is defined as $F_{\text{char}}=\frac{EI}{L^{2}}$. For the reference geometry, the code evaluates $F_{\text{char}}\approx 1.99\times10^{-5}\,\text{N}$. This load is applied downward in the z-direction at the tip. Simulation parameters are $T_{\text{total}}=5\,\text{s}$ and $\Delta t=0.1\,\text{s}$.

1) Time history of tip displacement

Figure 1 shows the axial tip displacement $\delta_z(t)$ versus time. The spring initially oscillates, overshooting the final displacement, then exhibits damped oscillations that decay due to numerical dissipation from the implicit scheme. The steady-state criterion flags convergence around t=3-4s, with a final displacement of approximately $\delta_z^{*}\approx-1.41\times10^{-3}\,\text{m}$. On the same plot, a dashed horizontal line at δ_z^{*} emphasizes the settled value.

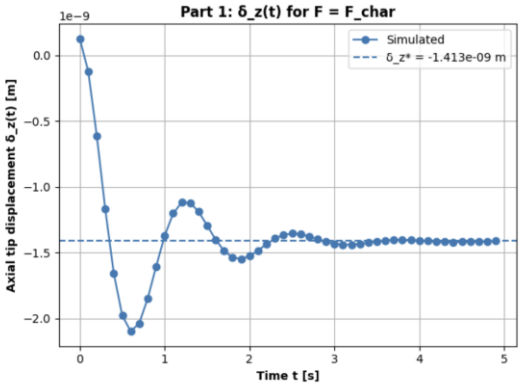

Figure1

2) Helix snapshots

At least five 3-D snapshots of the helix centerline are extracted and plotted using the set_axes_equal_3d helper so that the coil is not visually distorted. The clamped end is marked with a red triangle, and the free tip with a green triangle annotated by its z-coordinate (see example in the user's screenshot).

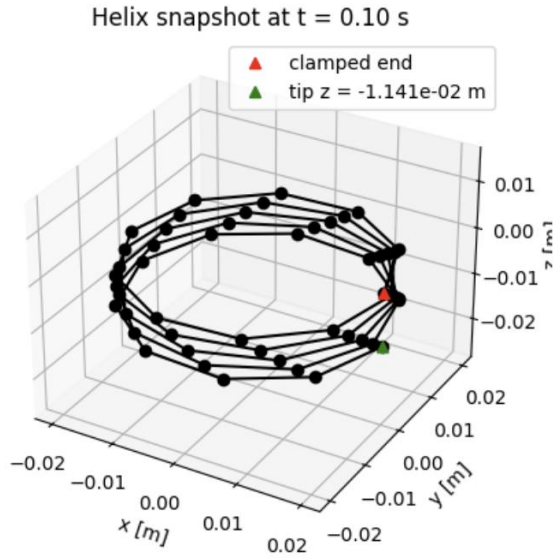

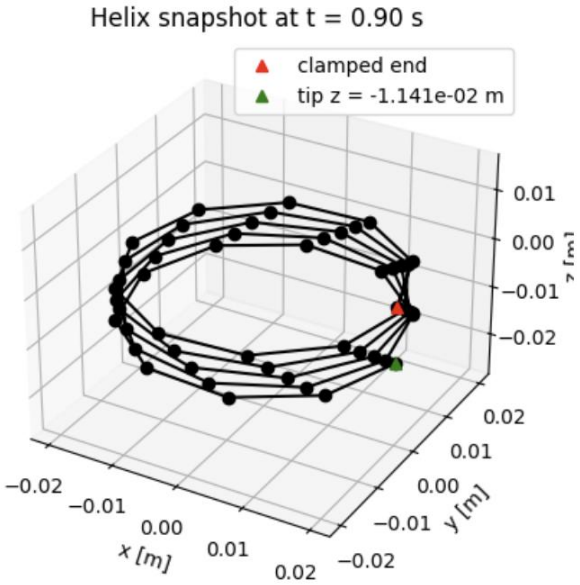

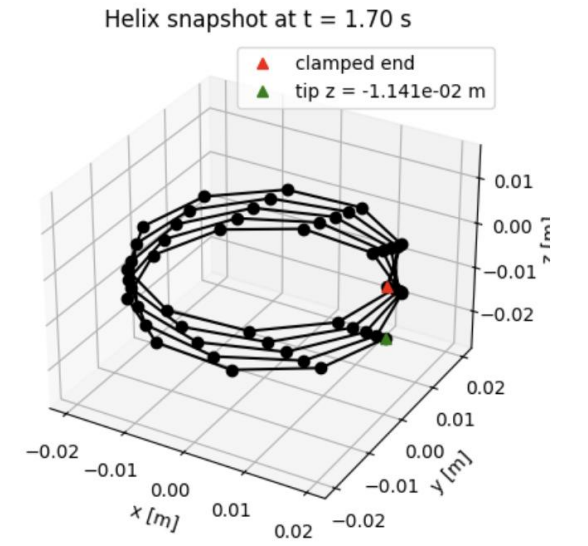

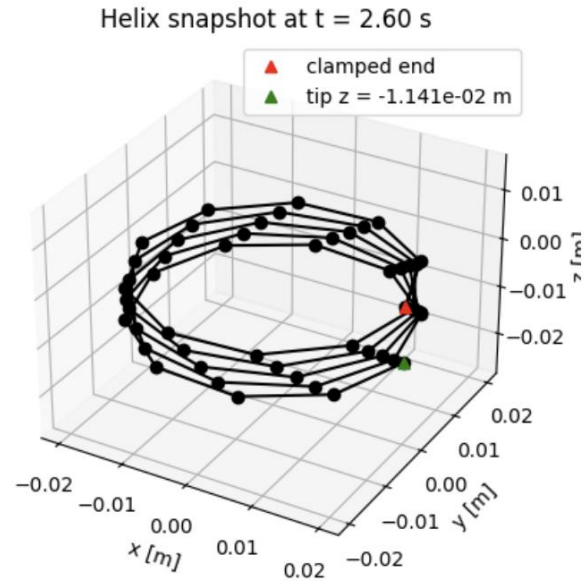

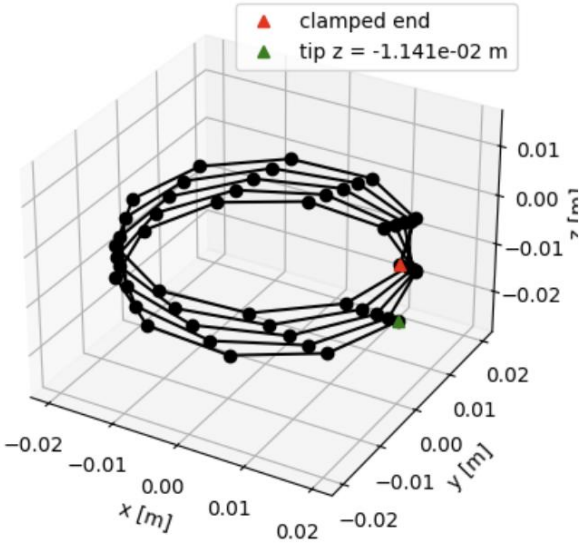

These snapshots visually confirm that the numerical solution reaches a smooth static equilibrium and that the chosen time step and tolerance are adequate.

B. Part 2 – Force Sweep and Linear Stiffness Fit

In Part 2, the same geometry is used while the tip load F is varied over 7 logarithmically spaced values between $0.01F_{\text{char}}$ and $10F_{\text{char}}$. For each force level, a longer total time (up to 20 s) and an optimized time step are used to ensure convergence, and the steady-state tip displacement $\delta_z^{*}(F)$ is recorded.

1) Force–displacement plot

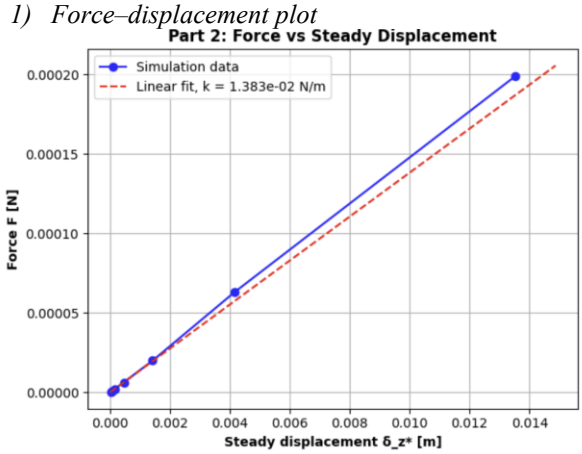

Figure 3 shows the simulation data F vs $|\,\delta_z^{*}\,|$ as blue markers and a best-fit line constraint to pass through the origin. Using the first half of the data (small-deflection regime) the fitted stiffness is

$$k_{\text{fit}} \approx 1.38 \times 10^{-2}\ \text{N/m}.$$

The data points lie very close to the fitted line for $|\,\delta_z^{*}\,| \lesssim 10^{-3}$ m, confirming nearly linear behavior in that range. At the largest force $10F_{\text{char}}$, the displacement magnitude increases to $\sim 1.35 \times 10^{-2}$ m; the point remains fairly close to the line, indicating that geometric nonlinearity is present but not extremely strong for the chosen geometry.

This part demonstrates that the DER model reproduces a well-defined effective spring constant in small deflections. The oscillatory transient is handled robustly by the dynamic relaxation, and the steady-state criterion avoids running unnecessarily long simulations for small forces. Any deviations from perfect linearity at larger forces reflect both geometric effects (the coil axis shortens, changing local curvature and torsion) and the fact that we are using a full 3-D beam model rather than the simplified torsional spring formula.

C. *Part 3 – Diameter Sweep and Comparison With Textbook Scaling*

For Part 3, the wire radius is kept fixed at $r_0 = 1$ mm, but the coil diameter D is varied linearly from 0.01 m to 0.05 m in ten steps. For each diameter, a mini force sweep with three forces between $0.01F_{\text{char}}$ and F_{char} is performed, and an effective stiffness $k(D)$ is extracted using a linear fit to F vs $|\delta_z^*|$.

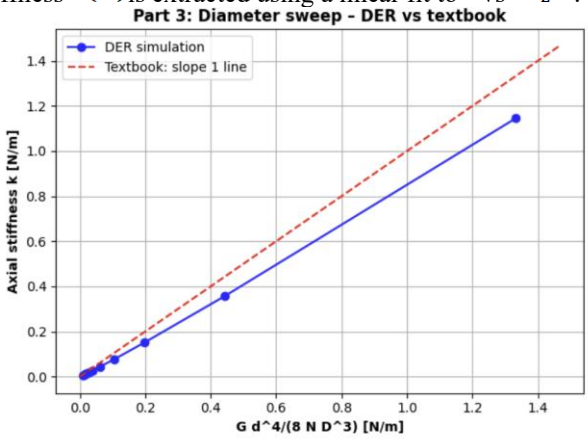

Figure 4 places the DER stiffness values k_{DER} on the vertical axis and the theoretical predictor $x(D)$ on the horizontal axis. The reference line $k = x$ (slope-1 dashed line) corresponds to perfect agreement with the textbook formula.
The DER points fall roughly along a straight line with slope slightly less than one. At smaller diameters (stiffer springs), the DER prediction is moderately lower than the textbook value; at larger diameters (more compliant springs), the difference is smaller but still noticeable. Overall, the trend confirms that the stiffness indeed scales approximately with D^{-3}, but the full beam model predicts a spring that is somewhat softer than the textbook torsion-only model.

III. Conclusion

This report used a Discrete Elastic Rod model to study the axial behavior of a helical compression spring. The main findings are:

1. Dynamic relaxation to equilibrium: Under a characteristic tip load F_{char}, the spring exhibits damped oscillations in tip displacement and reaches a steady state at $\delta_z^* \approx -1.4 \times 10^{-3}$ m. Multiple helix snapshots confirm smooth, physically reasonable deformations without numerical artifacts.

2. Effective linear stiffness: A log-spaced force sweep confirms a nearly linear relation between force and displacement in the small-deflection regime, yielding an effective stiffness $k_{\text{fit}} \approx 1.38 \times 10^{-2}$ N/m for the reference geometry.

3. Diameter dependence and theory comparison: When coil diameter is varied, the DER-computed stiffness values follow the expected D^{-3} scaling and align approximately, though not exactly, with the textbook torsion-based formula $k = Gd^4/(8ND^3)$. The DER model predicts slightly softer springs, reflecting additional deformation modes and finite-length effects.

References

[1] M. Khalid Jawed, MAE263F Lecture